Vol. 46, No. 1 (2024) 97-106, DOI: 10.24874/ti.1546.08.23.10

Tribology in Industry

www.tribology.rs

RESEARCH

Static and Kinetic Friction of 3D Printed Polymers and Composites

Nikolay Stoimenov[a,*], Mara Kandeva[b], Mihail Zagorski[b], Peter Panev[a]

[a]*Institute of Information and Communication Technologies – Bulgarian Academy of Sciences, Sofia, Bulgaria.*
[b]*Technical University of Sofia, Tribology Center, Sofia, Bulgaria.*

Keywords:

Polymeric materials
3D print technology
Tribology
Friction

* Corresponding author:

Nikolay Stoimenov
E-mail: nikistoimenow@gmail.com

Received: 21 August 2023
Revised: 12 September 2023
Accepted: 4 October 2023

A B S T R A C T

The work examines the characteristics of the static and kinetic friction of five types of polymer materials and composites obtained by 3D printing, which are united into 2 groups: group A: PLA, Tough PLA (Technical Polylactic acid), and SteelFill (PLA with stainless steel powder approx. w80%15) and group B: PETG (Polyethylene terephthalate): PETG and CarbonFil™ (PETG with carbon fibers). Results were obtained and analyzed for the variation of the static and kinetic friction force, the static and kinetic coefficient of friction (COF), and the difference between the static and kinetic COF (a jump in COF, known as Stick-slip) from the magnitude of the normal load in two cases of contact with a steel counter-body - without lubricant and with SAE15W40 oil.

1. INTRODUCTION

Grinding various materials to reduce their size is important for cement, pharmaceuticals, mining, food, and other fields of production. Grinding takes place in mills, which are divided into three main types: autogenous, semi-autogenous, and autogenous. In its essence, grinding is the destruction of materials under the influence of complex dynamic and contact processes such as shock, vibration, friction, wear, etc. The materials for the grinding bodies and the walls of the mill must combine a complex of alternative properties. On the one hand, they must have high hardness and strength to realize the destructive effects of impact interaction, and on the other hand, they must have high anti-wear and anti-friction properties, which is related to high plasticity. The details and mechanisms in the mills work in extreme operating conditions, where intensive processes of abrasive, erosive wear, corrosion, etc. take place. The processes are material-intensive and energy-intensive. Reducing energy intensity means reducing friction, which is inevitably present at the micro- and macro-level. Process studies in full-scale mills operating in production are expensive and require considerable time. With proper consideration of the operating factors, when modeling and simulating the movement and interaction of grinding bodies and grinding media,

data close to real can be obtained. The study of their tribological properties combined with the correct selection of the main factors would help to provide accurate input data when creating simulations with laboratory and production mills.

One of the methods of increasing the service life of contact elements and systems is the use of polymer, metal-polymer materials and coatings. Such materials combine the high mechanical strength inherent in metals with good anti-friction, anti-corrosion, anti-wear and other properties of modern polymers [1-10].

The rapid development and improvement of three-dimensional printing or 3D printing as a modern technology provides opportunities for the construction of high-tech materials and three-dimensional solid details. This technology is different in nature and has a number of advantages compared to conventional technologies. Most traditional modeling, creation, and manufacturing methods such as casting, forging, turning, milling, etc. are expensive, labor-intensive, and time-consuming for most users [11-16]. In work [17,18], the authors present a study and analysis of the main materials used in 3D print technologies. According to manufacturers, distributors, and market research, the main materials are PLA (polylactic acid), PETG (Polyethylene terephthalate), and ABS (Acrylonitrile butadiene styrene). Some of the other materials are ASA, TPE, TPU, TPC, PA, PC, PP, PEI, PVA, PVC, PEEK, HIPS, and others.

The majority of research on 3D polymers and composites has focused on their mechanical properties, which comprise about 12% of all research. Only 3% of these studies are related to their tribological properties [19].

The analysis of studies in the specialized literature in the field of tribology of 3D polymer materials and composites shows that they are related to the search for dependencies of the coefficient of friction and the intensity of wear on various factors such as normal load, sliding speed, roughness, the microhardness of polymers, the texture of the surface layer, the orientation and thickness of the layers [20-25]. The results are sometimes contradictory, and their comparison is associated with difficulties, and sometimes even impossibility, caused by the different methodologies and kinematic schemes of the tribotesters for research. The tribological processes of friction and wear are highly dependent on the design features of the tribotester – point contact between sphere and disk, linear contact between roller and disk, planar contact between thumb and disk, etc. For example, when studying the tribosystem "polymer ABS - steel 52100" under the kinematic scheme "sphere - disk" in dry friction, the coefficient of friction depends on the orientation of the surface layers relative to the sliding direction, mainly on the properties of these layers, and not on the roughness. However, the effect of these influences is highly dependent on the magnitude of the normal load [18]. Work [19] presents results on the wear characteristics of tribosystems containing biodegradable polymeric materials PLA built by FFF/FDM 3D printing. Results were obtained on the influence of 3D printing temperature and friction path on linear wear, wear intensity, and reciprocating wear resistance (reversible friction). In work [20], results are presented on the coefficient of friction and wear of PLA and PETG polymers in reciprocating forward sliding conditions without lubricant with different orientations of the layers and the structure of the print in the horizontal direction (X). The authors' finding is that the coefficient of friction, hardness, and wear depends on the thickness and orientation of the layers and the structure of the seal, but in a different way depending on the magnitude of the normal load.

It is of interest to improve the anti-friction and anti-wear characteristics of 3D polymers by introducing different additives with different amounts of shape and size - carbon, steel, nanodiamond, biocarbon, etc. [21,22,23]. Such polymers are called composites. It is necessary to carry out more in-depth and complex studies on the influence of technological factors on the tribological characteristics of these materials, such as static and kinetic coefficient of friction, parameters of wear and wear resistance in different operating modes - dry friction, boundary friction, abrasion, erosion, high sliding speeds, impacts, vibrations, etc. [24-27].

The object of the present work is to study the characteristics of static and kinetic friction of polymers and composites obtained by 3D printing, when the normal load changes in contact conditions without lubricant and contact with the lubricant. Specifically, static and kinetic friction force, static and kinetic coefficient of friction (COF), and the difference between static and kinetic COF (Stick-slip).

2. EXPERIMENTAL DETAILS

2.1 Materials

Five types of polymer materials and their composites obtained by 3D printing are studied, united into 2 groups: group A, which includes 3 types of polymer materials based on PLA (Polylactic acid): PLA, Tough PLA (Technical Polylactic acid) and Steelfill (PLA with stainless steel powder approx. w80%15); group B, which includes 2 types of polymer materials based on PETG (Polyethylene terephthalate): PETG and Carbonfil™ (PETG with carbon fibers).

Two cylindrical samples with a diameter of 10 mm and a height of 20 mm were made from each material. The horizontal surface of the samples, which is in contact with the steel counter body, is successively ground with sandpapers No. 320, 400, and 600 to a uniform roughness of Ra=0.123 μm. The roughness Ra is measured with an accuracy of 0.01 μm with a contact digital profilometer.

The microhardness of the samples was measured with a microhardness tester with a digital display model HVS-1000 under a load of 0.1 kg (0.981 N) with an indenter holding time of 10 s. Three measurements were made on each sample and their average value was taken. The density of the materials was determined as the ratio of the measured mass to the volume of each specimen. Sample numbering, designations, description, density, and microhardness data of the samples are shown in Table 1.

Figures 1 and 2 show density and microhardness diagrams of the test specimens.

From the analysis of the diagram in Figure 2, it can be seen that, of all the tested materials, the PETG polymer has the highest microhardness - 37 Vickers units, and the PLA polymer - 18 units have the lowest, despite the close values of their densities. This is probably due to their nature, molecular structure, and different viscoelastic properties.

The introduction of additional components into 3D polymer materials changes their microhardness differently. The three composite polymers Tough PLA, Steelfill and Carbonfil™ have almost the same microhardness of 26-27 units, which is higher than the microhardness of PLA and lower than that of PETG polymer. The value of the microhardness of the polymer composites depends on the parameters of the technological mode during their printing.

Table 1. Designation, description, density, and density of the tested materials.

Sample		Designation	Description
A Group	1	A1-PLA	Polylactic acid
	2	A2-Tough PLA	Technical Polylactic acid
	3	A3-Steelfill	PLA with stainless steel powder approx. w80%15
B Group	4	B4- PETG	Polyethylene terephthalate
	5	B5-Carbonfil™	PETG with carbon fibers

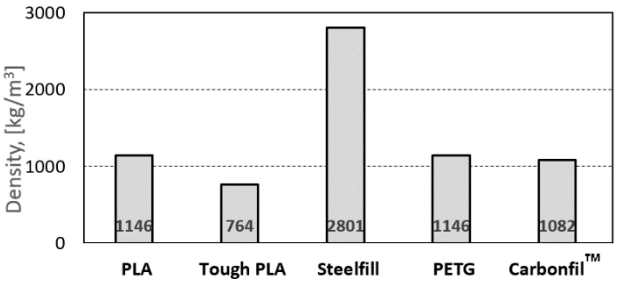

Fig. 1. Density diagram of the tested materials.

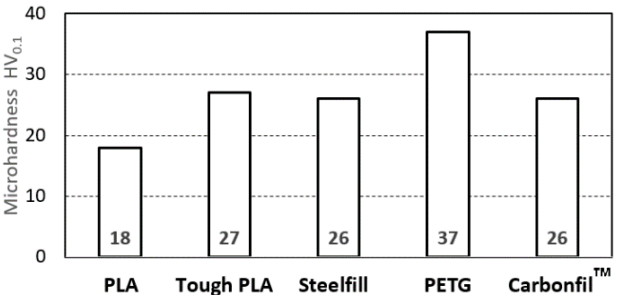

Fig. 2. Diagram of the hardness of the tested materials.

2.1. Device and methodology

The static and kinetic friction forces are measured with a tribotester, the functional scheme of which is presented in Fig. 3. The tribosystem consists of sample 1 (body), which is fixed in holder 3, and a fixed counter body 2. The design of the holder allows samples of different shapes and sizes to be fixed. The normal load P is set using a lever system or weights 4, to guarantee a uniform distribution of contact pressure over the entire nominal contact area between the body and the counter body. The normal load is shown in the diagram as a concentrated force P at the center of gravity of the nominal contact pad.

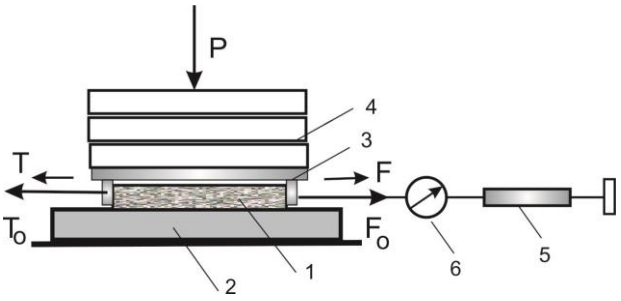

Fig. 3. Functional diagram of a tribotester for static friction research: 1-sample; 2-antibody; 3-sample holder; 4-weights; 5-micrometer screw; 6-dynamometer.

Specimen 1 is connected to a dynamometer 6 and a micrometer screw 5 by means of an inelastic thread attached to the holder 3. The lower surface of holder 3 is located at a distance of 2 mm above the contact surface of contact between the specimen and the counter body. The measurement of the static friction force is carried out in the following sequence: sample 1 is fixed in the bed of holder 3 and a certain load P is set. The time of stationary contact at the set load is recorded with a stopwatch. The scale of the dynamometer 6 is zeroed and by slowly moving the micrometer screw a tangential force F is smoothly applied to specimen 1. The value of the force F is read on the scale of the dynamometer 6, tared in Newtons. The Force F tends to move sample 1 to the right along the surface of the counter body 2. At small values of the force F, the sample maintains an apparent state of rest. Upon reaching the limit value Fo, even with the smallest increase in force, the specimen goes into motion. At this point, a decrease in the value of the force F is observed.

The limiting force of friction is known in classical mechanics as a static frictional force. In modern tribology, it is the maximum frictional force generated by preliminary micro displacements in the contact during the transition of the tribosystem from a state of rest to apparent motion (Figure 4). It is determined by the condition for the equilibrium of the tribosystem:

$$T_o = F_o \quad (1)$$

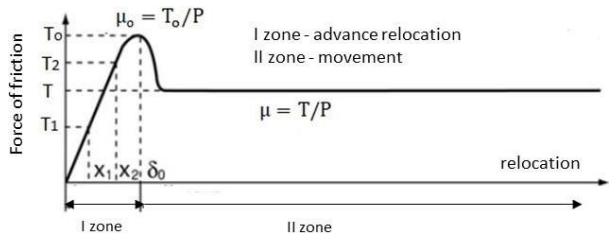

Fig. 4. Change in frictional force from rest to motion.

The magnitude of the force To is measured by the maximum reading of the dynamometer, after which its value decreases and remains constant. This value represents the magnitude of the kinetic friction force T during the movement of the specimen. The static μ_o and kinetic μ coefficient of friction (COF) are determined by the Leonardo-Amonton law of frictional forces, respectively:

$$T_o = \mu_o P \quad \text{and} \quad T = \mu P \quad (2)$$

and

$$\mu_o = \frac{T_o}{P}; \quad \mu = \frac{T}{P} \quad (3)$$

The difference between static and kinetic COF $\Delta\mu = \mu_o - \mu$ represents the COF spike when sliding, also known as Stick-slip. Briefly, the research methodology consists of measuring the static and kinetic friction forces and calculating the static, kinetic COF, and COF jump.

3. EXPERIMENTAL RESULTS AND ANALYSIS

With the described device and methodology, results were obtained for the static and kinetic friction forces at several values of the normal load: 30 N, 40 N, 50 N, 60 N, and 70 N in two cases - contact without lubricant and contact with SAE mineral oil 15W40.

3.1. Effect of normal load on frictional forces

Figures 5 and 6 show the dependences of the variation of the static friction force on the normal load in the cases of contact without lubricant and with lubricant for both groups A and B polymers and composites.

Comparing the two pure 3D polymers PLA and PETG, it was found that at small values of the load (P=30N), the static friction forces have very close values – 9N and 8 N. When the load increases 2.3 times (P=70N) the static force of friction of PLA polymer increases by 55% and static friction force of PETG polymer increases by 150%. The two polymers have the same density (1145.91 kg/m^3), but their microhardness is different: PETG polymer has more than twice the microhardness (HV0.1=37.2) than the microhardness of PLA (HV0.1=18.2).

Comparing the group A polymer composites at maximum load, it can be seen that the static friction force of the Tough PLA composite is the greatest, which is 21% greater than that of the pure PLA polymer. The static strength of the Steelfill composite is the lowest, which has lower values than that of the pure PLA polymer by 14%. In short, PLA polymer modification affects the static strength at high load in dry friction mode differently, i.e., it can lead to its increase or decrease (Fig.5).

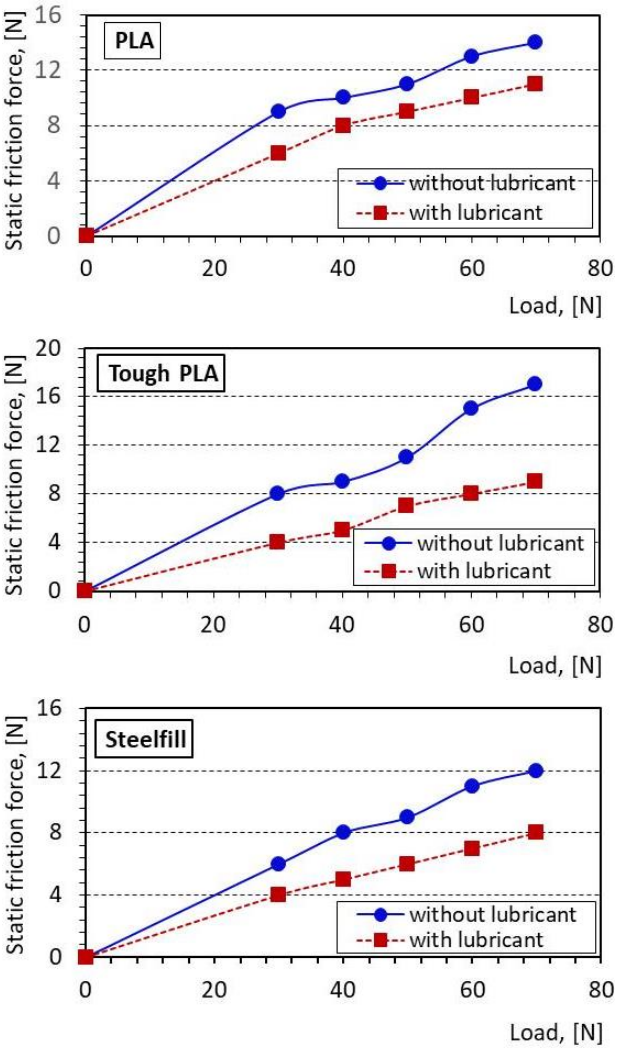

Fig. 5. Variation of static frictional force from normal loading for group A materials.

For the materials of group B, it is noticeable that polymer PETG has a sharp increase in static force after a certain load value (P=50N). The modification of PETG with graphite fibers leads to two findings: first - a linear variation of the static force with the load and second - at high load, the static friction force decreases by 35% compared to that of the pure PETG polymer (Fig. 6).

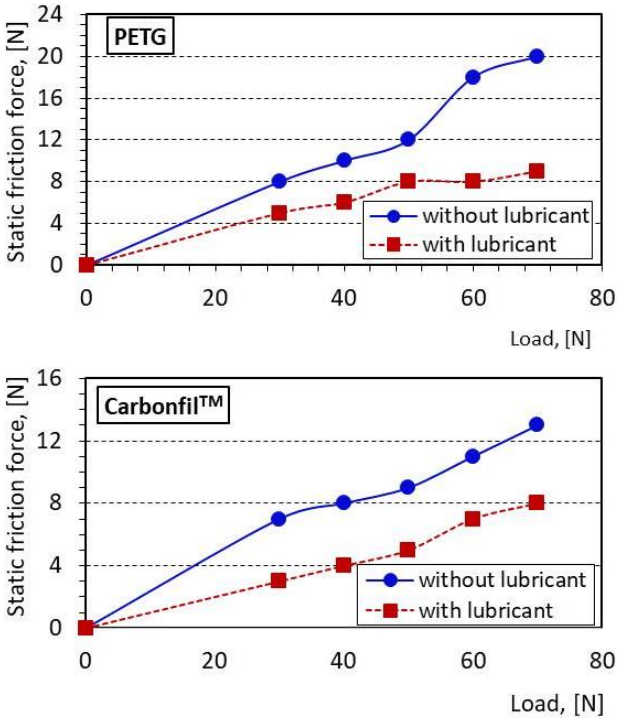

Fig. 6. Variation of static frictional force from normal loading for group B materials.

3.2. Effect of normal load on frictional forces

Plots of static COF variation with load for Group A and Group B materials in unlubricated and oiled contact are presented in Figures 7 and 8.

For composite polymers of group A, the variation of COF with loading has different character and absolute values. For Tough PLA polymer, the curve has a wavy character. Up to a certain load value (50N), the COF decreases, reaches a minimum, then increases to values higher than those of pure PLA polymer at a load of 60N, and starts to decrease again. Such load instability of COF is not observed in composite with metal particles (Steelfill) - fig. 7.

For the Carbonfil™ composite polymer of Group B, in dry friction, the change in COF with load has a persistent character, and at high load, it reaches values 38% lower than the COF of the pure PETG polymer. In contact with oil at a high load, both materials have the same COF (Fig.8).

Figures 9 and 10 present diagrams of the static and kinetic COF of all investigated materials under the normal load of 30 N, 50 N, and 70N in contact without and with lubricant.

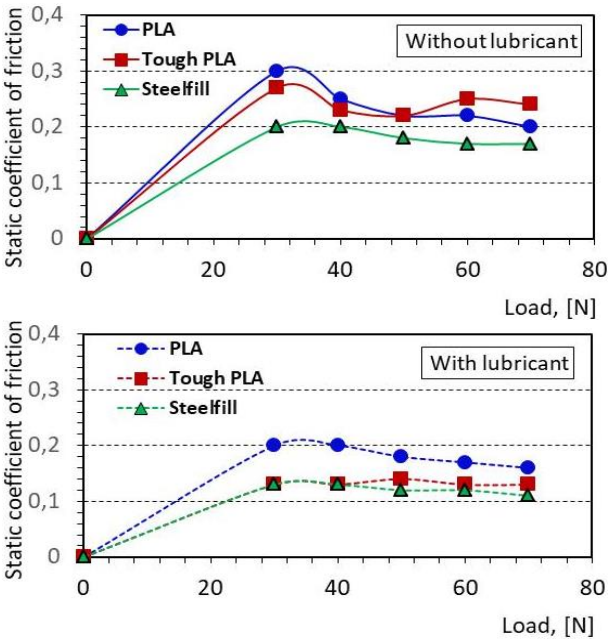

Fig. 7. Variation of static coefficient of friction by loading of group A polymers and composites.

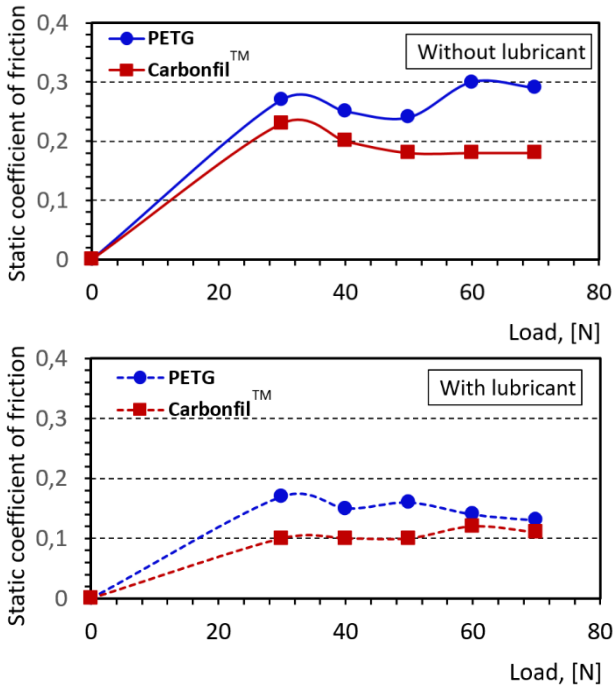

Fig. 8. Variation of static coefficient of friction by loading of group B polymers and composites.

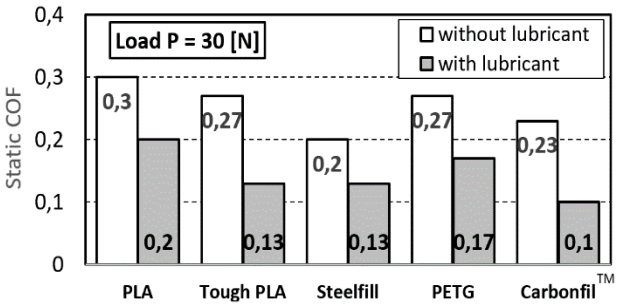

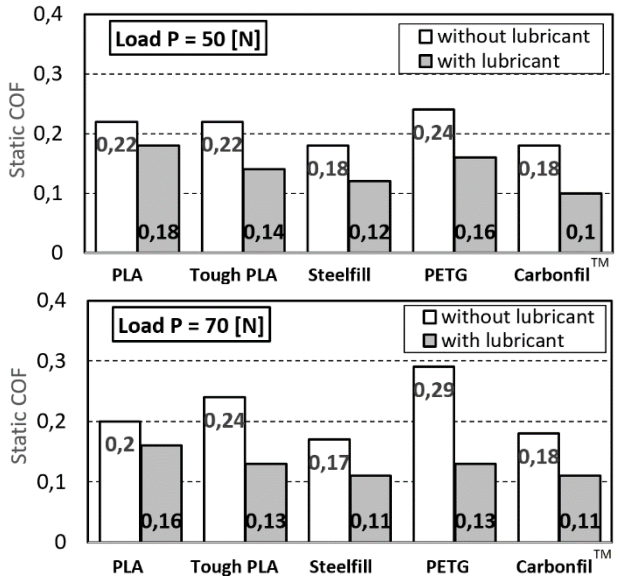

Fig. 9. Diagrams of the static COF of the tested materials under different loading.

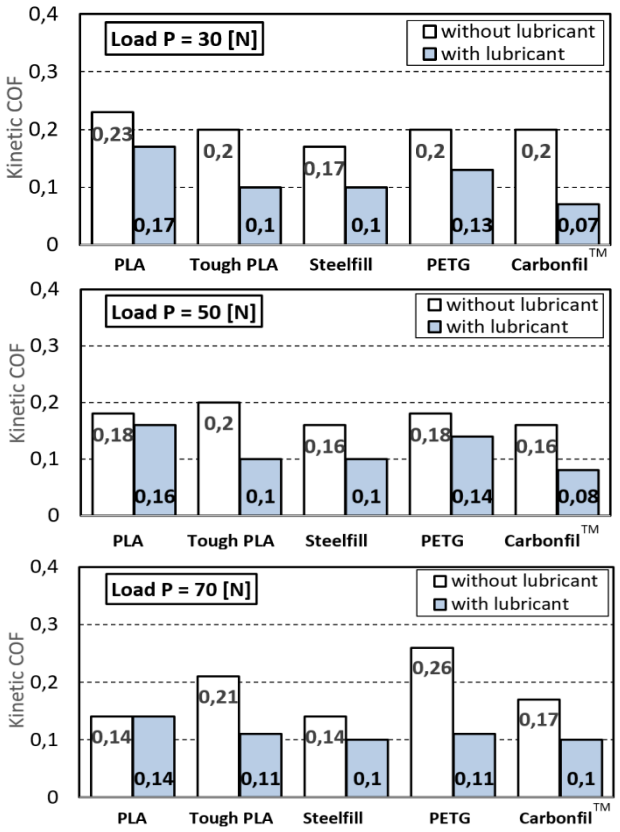

Fig. 10. Diagrams of the kinetic COF of the tested materials under different loading.

3.3. Influence of the normal load on the jump of the coefficient of friction

Figure 11 shows plots of the COF jump for each of the tested polymers and composites at three load values - 30N, 50N, and 70N, in both non-lubricated and lubricated contact cases.

The analysis of the diagrams from Fig. 11 shows the following: at a small load - 30 N, the largest jump in COF (30%) is observed for Carbonfil composite in contact with oil, which, when increasing the load 50 N and 70 N, decreases by the same value (9.1%). The high jump in lubricated contact can be explained on the one hand by the penetration and interaction of the lubricant with the surface layer of the composite polymer and the possibility of breaking the long polymer chains. Due to the presence of graphite fibers, adsorption, and capillary processes occur, which further lead to an increase in the COF spike. On the other hand, in the process of preliminary displacement, mechanical elastohydrodynamic interactions are possible in the contact gap, which leads to an additional increase in static friction losses.

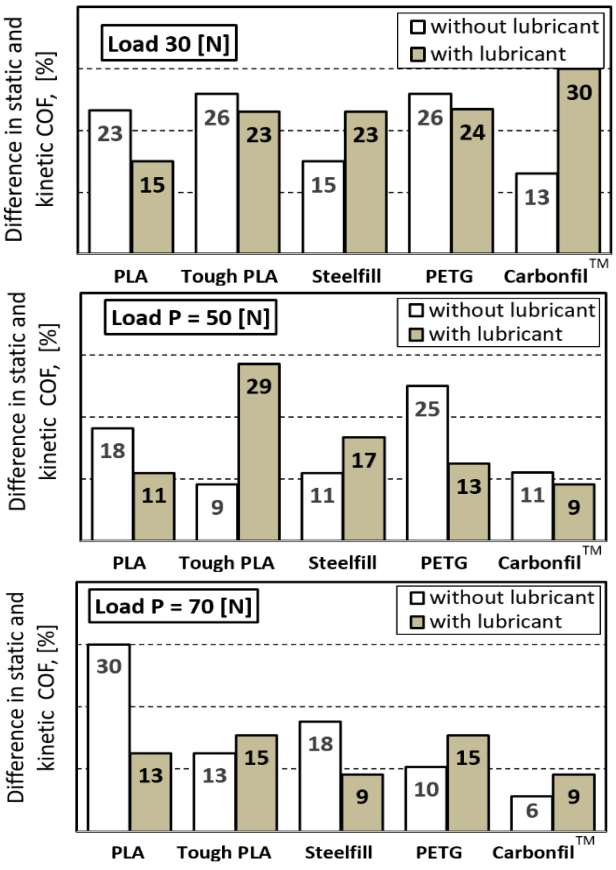

Fig. 11. Diagrams of the difference between the static and kinetic COF of the test materials under different loading.

The high COF value (30%) of PLA polymer in oil-free contact at high load is due to the high elastic contact characteristics due to the deformation component of friction. Close values of the COF jump (28.6%) were observed for Tough PLA composite in lubricated contact at average load values - 70 N.

At high load, except for PLA polymer, all other tested materials show low and close COF jump values: in lubricated contact in the range of 9.1% to 15.4%, and in dry contact – from 5.6% to 17.6%. Changes in the COF jump within these limits are acceptable and do not significantly affect the stability of the tribosystem, its vibration state, and the danger of shocks, which is of great importance not only for the coefficient of useful action but also for the intensity of wear.

The analysis of the results obtained in the present study is based on the current generally accepted molecular-mechanical (adhesion-deformation) theory of friction. According to this theory, friction is a phenomenon that has a dual nature. Its quantitative characteristics such as force and coefficient of friction are presented as a sum of two components – molecular (adhesion) and mechanical (deformation). The two components make different contributions to the friction mechanisms depending on the complex combinations of a number of factors. It should be noted here that the mechanisms of frictional contact interactions in the polymer-metal system are essentially different from the mechanisms of friction in the metal-metal system. A specific feature of contact as a third body in any tribosystem is its discrete structure. It is expressed in the presence of microcontact formations (contact spots) that form the actual contact area. The main triboprocesses of friction and wear take place in the actual contact area of contact and are related to lubrication, contact conductivity (thermal conductivity, electrical, gas-hydraulic, etc.), and capillarity by a very complex mechanism.

The force of friction is proportional to the actual contact area. At small values of the normal load, the molecular component of friction dominates, i.e. atomic-molecular interactions and the force of friction has smaller values. Here we must emphasize that the static friction force and the friction jump, in addition to the load, the roughness of the counter body, the nature, structure, and viscosity of the lubricant, significantly depend on the duration of the static contact, i.e. from the action time at the corresponding load. Our research was conducted with the same duration of the load - 120 seconds. As the load increases, the actual contact area increases and the friction force increases due to an additional component of hysteresis processes

caused by the viscoelastic properties of the polymers. Many authors assume that the deformation component of friction is negligibly small compared to the hysteresis component and in most cases neglect it. This is likely to be the case for polymers with very low modulus. In the case of 3D polymers and their modification with different components, due to the increased mechanical properties, not only elastic but also elastoplastic and plastic deformations are possible. As the load increases, the atomic-molecular component decreases, while the hysteresis and deformation components increase. Here we should also note the fact that in the "metal-metal" contact system, micro-contacts with high adhesion strength are formed between the tips of the roughnesses, while in the "polymer-metal" system, due to the specificity of its structure and elastic properties, the polymer surrounds the roughnesses of the metal. In the process of preliminary movement in the tribosystem, the polymer layer in front of the metal roughness is subjected to tension, and after it - to pressure. The magnitude of the static frictional force depends on the elastic characteristics of the polymer – modulus of elasticity, tensile strength yield strength, etc. At this stage, this explains the fact that when rubbing PETG polymer under high load, the static friction force is 2.5 times greater than that of PLA polymer. This is due to the low value of the modulus of elasticity (2020 MPa) and yield strength (50 MPa). The low value of the modulus of elasticity implies large relative deformations, correspondingly a larger actual contact area of contact, which in turn leads to an increase in the static frictional force. PLA polymer has a higher modulus of elasticity of 3120 MPa, which results in smaller elastic and hysteresis losses.

The incorporation of metal and carbon components of different sizes, shapes, amounts, and orientations in the polymer 3D polymers affects the contact forces and interactions in the process of preliminary micro displacements in a different way.

4. CONCLUSION

In the work, the characteristics of the static and kinetic friction of five types of polymer materials and composites obtained by 3D printing, are united into 2 groups: group A includes 3 types of materials based on PLA (Polylactic acid): PLA, Tough PLA (Technical Polylactic acid) and Steelfill (PLA with stainless steel powder approx. w80%15) and group B, which includes 2 types of polymer materials based on PETG (Polyethylene terephthalate): PETG and Carbonfil™ (PETG with carbon fibers). Results were obtained for density, microhardness, change in static and kinetic friction force, static and kinetic coefficient of friction (COF), and the difference between static and kinetic COF (COF jump) from the magnitude of the normal load - 30 N, 40 N, 50 N, 60 N and 70 N in two cases of contact with a steel body - without lubricant and with engine oil SAE15W40.

It was found that:

- In unlubricated friction, for all materials, the static friction force has higher values than the static friction force in contact with oil.
- The static friction force in contact without lubricant increases non-linearly with increasing normal load, and in contact with lubricant, the dependence is linear. This nonlinearity is more pronounced for group B polymers, especially PETG polymer and its Carbonfil™ composite. During dry friction of the pure 3D polymers PLA and PETG at small load values (P=30N) the static friction forces have very close values - 9N and 8 N, but when the load increases 2.3 times (P=70N) the static friction force of PLA polymer increases by 55% and static friction force of PETG polymer increases by 150%.
- A general trend for all tested materials is a decrease in COF with increasing load. In dry rubbing of the 3D polymers PLA and PETG, the dependence has a different character. For PLA, the COF decreases smoothly with increasing load and at the highest load reaches values lower than those of Tough PLA composite. For PETG polymer, the COF dependence on load has a wavy character with alternating maxima and minima. At high load, the COF of static friction of PETG reaches 50% higher values than that of PLA.
- Modification of the studied 3D polymers PLA and PETG with metal and carbon components in most cases leads to a decrease in static and kinetic COF with increasing load in contact without and with oil.

- For composite polymers of group A, the variation of COF with loading has different character and absolute values. For Tough PLA polymer, the curve has a wavy character with alternating minima and maxima. Such loading instability of COF is not observed in composite with metal particles (Steelfill).
- In the composite polymer Carbonfil™ of group B, during dry friction, the variation of COF with the load has a persistent character and at high load, it reaches values 38% lower than the COF of the pure PETG polymer. In contact with oil at a high load, both materials have the same COF values.

Acknowledgment

This research was carried out as part of project No. KP-06-N47/5 "Research and optimization of the interaction between grinding bodies and media with an innovative shape", financed by the Bulgarian National Science Fund.

REFERENCES

[1] N. Stoimenov, D. Karastoyanov, and L. Klochkov, "Study of the factors increasing the quality and productivity of drum, rod and ball mills," AIP Conference Proceedings, Jan. 2018, doi: 10.1063/1.5060704.

[2] *Innovations, European, national and regional policies*, Applied Research and Communications ARC FUND (In Bulgarian), 2008.

[3] D. Karastoyanov, N. Stoimenov, *Lifter*, Patent of Bulgaria, Reg. No. 67020/28.01.2020

[4] R. Gras, *Tribologie, Principes et Solutions Industrielles*, L'usine nouvelle, Dunod, 2008.

[5] R. Bassani, *Tribology*, Pisa University Press, Technology & Engineering Mechanical, 2013.

[6] N. Denisova, V. Shorin, I. Gontar, N. Volchikhina, N. Shorina, Tribotechnical Materials Science and Tribotechnology, Penza, (in Russian), 2006

[7] T. Penyashki *et al*., "Some Ways to Increase the Wear Resistance of Titanium Alloys," *Journal of the Balkan Tribological Association*, vol. 27, no. 1, pp. 1–20, Feb. 2021.

[8] M. K. Kandeva, Z. Kalitchin, and Y. Stoyanova, "Influence of chromium concentration on the abrasive wear of Ni-Cr-B-SI coatings applied by supersonic flame jet (HVOF)," in *Vide Leaf, Hyderabad eBooks*, Jan. 2021. doi: 10.37247/pams2ed.3.2021.30.

[9] M. K. Kandeva, N. Stoimenov, B. I. Popov, Z. Kalitchin, and V. Pozhidaeva, "Abrasive wear resistance of micro- and Nano-Diamond particles," *Journal of the Balkan Tribological Association*, vol. 26, no. 2, pp. 193–205, Jan. 2020.

[10] V. Dyakova, P. Tashev, and M. K. Kandeva, "Study on the effect of nanosized particles of tin and SIC on the wear resistance, microstructure and corrosion behavior of overlay weld metal," *Journal of the Balkan Tribological Association*, vol. 26, no. 1, pp. 56–65, Jan. 2020.

[11] N. K. Myshkin, M. I. Petrokovets, *Tribology. Principles and Applications*, IMMS NASB, Gomel, (in Russian), 2002.

[12] D. Moore, *The Friction and Lubrication of Elastomers*, Pergamon Press, 1977.

[13] N. K. Myshkin, C. K. Kim, M. I. Petrokovets: *Introduction to Tribology*, Seoul: Cheong Moon Gak, 1997.

[14] Create it REAL Aps., available at: https://www.createitreal.com/3d-printer-electronics/48/, accessed: 20.03.2023.

[15] S. Farah, D. G. Anderson, and R. Langer, "Physical and mechanical properties of PLA, and their functions in widespread applications — A comprehensive review," *Advanced Drug Delivery Reviews*, vol. 107, pp. 367–392, Dec. 2016, doi: 10.1016/j.addr.2016.06.012.

[16] B. Popov, M. Paneva, N. Stoimenov, L. Klochkov, Survey and analysis of materials for 3d printing, XXX International Scientific and Technical Conference, ADP - 2021., Sozopol, Bulgaria., Publishing house of TU-Sofia, Publisher Department "Automation of Discrete Production Engineering" Mechanical Engineering Faculty, Technical University - Sofia, pp. 218-221.

[17] 3D Jake, available at: https://www.3djake.com/, accessed: 20.03.2023.

[18] M. A. Ramadan "Tribological Investigations of 3D printed polymers and their Applications: a review," *Journal of Modern Industry and Manufacturing*, vol. 1, no. 1, pp. 1-9, Mar. 2022, doi: 10.53964/jmim.2022002.

[19] F. Dangnan, C. Espejo, T. Liskiewicz, M. Gester, and A. Neville, "Friction and wear of additive manufactured polymers in dry contact," *Journal of Manufacturing Processes*, vol. 59, pp. 238–247, Nov. 2020, doi: 10.1016/j.jmapro.2020.09.051.

[20] M. Zagorski, G. Todorov, N. Nikolov, Y. Sofronov, and M. K. Kandeva, "Investigation on wear of biopolymer parts produced by 3D printing in lubricated sliding conditions," *Industrial Lubrication and Tribology*, vol. 74, no. 3, pp. 360–366, Mar. 2022, doi: 10.1108/ilt-06-2021-0214.

[21] S. Z. Hervan, A. Altınkaynak, and Z. Parlar, "Hardness, friction and wear characteristics of 3D-printed PLA polymer," *Proceedings of the Institution of Mechanical Engineers, Part J: Journal of Engineering Tribology*, vol. 235, no. 8, pp. 1590–1598, Oct. 2020, doi: 10.1177/1350650120966407.

[22] E. G. Ertane, A. Dorner-Reisel, Ö. Baran, T. Welzel, V. Matner, and S. Svoboda, "Processing and Wear Behaviour of 3D Printed PLA Reinforced with Biogenic Carbon," *Advances in Tribology*, vol. 2018, pp. 1–11, Aug. 2018, doi: 10.1155/2018/1763182.

[23] P. H. M. Cardoso, M. F. L. De Oliveira, M. G. Oliveira, and R. M. Da Silva Moreira Thiré, "3D Printed Parts of Polylactic Acid Reinforced with Carbon Black and Alumina Nanofillers for Tribological Applications," *Macromolecular Symposia*, vol. 394, no. 1, Dec. 2020, doi: 10.1002/masy.202000155.

[24] T. Grejtak et al., "Whisker orientation controls wear of 3D-printed epoxy nanocomposites," *Additive Manufacturing*, vol. 36, p. 101515, Dec. 2020, doi: 10.1016/j.addma.2020.101515.

[25] M. Kandeva, N. Stoimenov, M. Paneva, "Abrasive Wear of Polymer Composite Materials Obtained by 3D Print Technology, Part I. Polymer Materials," *Journal of the Balkan Tribological Association*, vol. 28, no. 3, pp. 362–379, 2022.

[26] M. Kandeva, N. Stoimenov, G. Kotseva, "Abrasive Wear of Polymer Composite Materials Obtained by 3D Print Technology. Part II. Composite Polymer Materials," *Journal of the Balkan Tribological Association*, vol. 28, no. 4, pp. 469–480, 2022.

[27] M. Zagorski, "Investigation on Abrasive Wear of Biodegradable Thermoplastic Polymer Samples Produced by FFF/FDM 3D Printing," *Journal of the Balkan Tribological Association*, vol. 28, no. 4, pp. 481–488, 2022.